



HAL
open science

Coherent beam combining of lasers: toward wavelength versatility and long-range operation compliance

Pierre Bourdon, Rodwane Chtouki, Laurent Lombard, Anasthase Liméry, Juline Le Gouët, François Gustave, Hermance Jacqmin, Didier Goular, Christophe Planchat, Anne Durécu

► To cite this version:

Pierre Bourdon, Rodwane Chtouki, Laurent Lombard, Anasthase Liméry, Juline Le Gouët, et al.. Coherent beam combining of lasers: toward wavelength versatility and long-range operation compliance. XXIII International Symposium on High Power Laser Systems and Applications, Jun 2022, Prague, Czech Republic. pp.12, 10.1117/12.2656457 . hal-04102307

HAL Id: hal-04102307

<https://hal.science/hal-04102307v1>

Submitted on 30 May 2023

HAL is a multi-disciplinary open access archive for the deposit and dissemination of scientific research documents, whether they are published or not. The documents may come from teaching and research institutions in France or abroad, or from public or private research centers.

L'archive ouverte pluridisciplinaire **HAL**, est destinée au dépôt et à la diffusion de documents scientifiques de niveau recherche, publiés ou non, émanant des établissements d'enseignement et de recherche français ou étrangers, des laboratoires publics ou privés.

Coherent Beam Combining of Lasers: Toward Wavelength Versatility and Long-Range Operation Compliance

Pierre Bourdon*, Rodwane Chtouki, Laurent Lombard, Anasthase Liméry, Julien Le Goüet, François Gustave, Hermance Jacquemin, Didier Goular, Christophe Planchat, Anne Durécu
ONERA, The French Aerospace Lab, Theoretical and Applied Optics Department (DOTA),
BP 80100, 91123 Palaiseau cedex, France

ABSTRACT

Coherent beam combining (CBC) by active phase control is an efficient technique to power scale fiber laser sources emitting in the near-infrared, between 1 and 2 μm , up to the multi-kilowatt level. Interestingly, it has been demonstrated by our team that CBC could also be used to power scale mid-infrared sources, frequency converters, generating a wavelength between 3 and 5 μm . We present our latest results on coherent combining of continuous-wave high-efficiency mid-infrared sources: optical parametric oscillators (OPOs) and detail the difficulties encountered to achieve this combining, as well as the main limitations to efficient operation of CBC in this case.

In a second part of this talk, we also present recent results on coherent combining of seven 1.5- μm fiber lasers through active phase control, using frequency-tagging, and operating efficiently on a remote target. A testbed has been designed to combine these 7 lasers on a remote surface, with phase-locking operating through analysis of the optical signal back-scattered by the target, in a so-called target-in-the-loop (TIL) experiment. In such TIL configuration, CBC mitigates both laser-amplification-induced and atmospheric turbulence-induced phase fluctuations simultaneously. CBC demonstrated proper operation outdoors, on a target located up to 1 km from the laser and the results from this experimental campaign will be described.

Keywords: Fiber laser, Coherent Beam Combining, nonlinear optics, Optical Parametric Oscillator, phase control, turbulence mitigation

1. INTRODUCTION

Coherent beam combining (CBC) techniques involving active phase control of the laser emitters have demonstrated their potential to power scale continuous-wave [1] and pulsed [2] fiber lasers through coherent addition of the power emitted by multiple separate amplifiers. Using all-fiber components, very compact configurations of coherently combined fiber amplifiers can be designed, with demonstrated overall emitted power exceeding the kilowatt level [1].

However, high power fiber lasers are only available within a finite set of wavelengths, mainly amongst 1 μm , 1.5 μm and 2 μm . Hopefully, nonlinear crystals offer the capability to convert these laser lines to access higher wavelengths in the midinfrared bands, for instance around 4 μm . But as with lasers, power scaling of frequency converters is limited, essentially by the damage threshold of the nonlinear medium. Coherent combining techniques could be useful to power scale frequency converters beyond this damage threshold limit. Unfortunately, combination techniques are difficult to implement in this case, as active phase control requires fast phase modulators at the midinfrared wavelength emitted by the converter. Such components are not exactly "off-the-shelf" and are not as practical nor as fast as the all-fiber modulators available at more standard wavelengths.

Taking advantage of the phase-matching relations involved in any frequency converting process, one can indirectly control the converted wave phase through control of the pump wave phase. When this pump wave is delivered by fiber amplifiers, such a frequency-converter coherent combining configuration can be achieved using standard off-the-shelf all-fiber phase modulators.

* pierre.bourdon@onera.fr; phone (+33) 1 80 38 63 82; fax (+33) 1 80 38 63 45; www.onera.fr

Our team successfully applied this approach to perform efficient coherent combination of second harmonic generators and difference frequency generators [3], [4], [5]. In a first part of this paper, we present the challenges of extending this indirect phase control technique to midinfrared OPO coherent combining, as well as the main limitations to efficient operation of CBC in this case. An experimental test of OPO CBC is also detailed.

CBC has been demonstrated for a large number of lasers [6], [7], but many realizations use the fact that the laser beams are spatially separated at the output of the lasers, before overlapping after propagation and becoming undistinguishable. While the laser beams are still spatially distinct, it's feasible to measure the phase of each laser and to control this phase in real time to achieve phase-locking. However, for some applications, such process cannot be applied as phase measurement has to be done once the laser beams have already begun to overlap and to interfere.

That's the case of target-in-the-loop CBC where one wants to phase-lock the lasers on a remote target, maximizing the power density deposited at long range. In this case, phase measurement at the output of the lasers is useless, as beam propagation induces additional phase shifts that are not accounted for in this measurement. It's necessary to find some way of driving the laser phases, benefiting from the information available in the optical signal backscattered by the remote target.

One approach is to try and maximize the intensity of this backscattered signal, as maximum power density deposited on the target corresponds to a maximum of this backscattered signal too. It's been done, for instance, very early on, during the first experiments of TIL-CBC on a glint target [8], and, later on, up to 7 km using a stochastic parallel gradient descent algorithm [9], a classical approach to maximize optical intensity by step-by-step optical wavefront correction.

In 2009, our team demonstrated a more practical and promising approach that can be performed using frequency-tagging for CBC phase control [10]. Frequency-tagging each optical channel at a specific frequency to assess the phase fluctuations to be compensated for is an efficient technique for CBC, also known as LOCSET [11]. Frequency-tagging has the advantage of "engraving" specific information on the signal emitted by each optical channel through low-depth modulation. This tagging process enables to easily retrieve the phase information from each channel, within the complex interference signal generated once the laser beams have overlapped. Moreover, this phase information retrieval can also be achieved using the backscattered signal from a remote target. We also demonstrated that a simple evolution of the configuration of detection used for direct CBC could transform a standard CBC system into a fully operational TIL-CBC device [10].

The tests we performed in 2009 were in the laboratory with artificially generated atmospheric turbulence. In a second part of this paper, we present the work done recently to build a testbed coherently combining seven 1.5- μm fiber lasers through active phase control, using frequency-tagging. We also present the first results obtained on TIL-CBC operating this testbed. These results are obtained propagating the laser beams through the atmosphere, hence through real atmospheric turbulence over a distance ranging up to 1 km.

2. COHERENT COMBINING OF OPTICAL PARAMETRIC OSCILLATORS

2.1 Principle and experimental setup for CBC of parametric amplifiers

Coherent beam combining of non-degenerate three wave mixing nonlinear processes was first demonstrated on devices that didn't require a cavity to operate: difference frequency generators.

But the theoretical bases are identical to those of OPO CBC, as both experiments combine parametric amplifiers.

To achieve CBC of DFGs or OPOs, phase control of one of the converted waves, the signal or the idler waves, has to be performed. Indirect phase control benefits from the phase-matching condition.

The electric field corresponding to each nonlinearly coupled wave can be written as:

$$\tilde{\mathbf{E}}_m(\mathbf{z}, t) = A_m(\mathbf{z})e^{jk_m z}e^{-j\omega_m t} + c. c \quad (1)$$

with $m = s, i$ or p and A_m the complex amplitude of the ω_m pulsation wave.

If we assume that the pump wave is not depleted when passing through the crystal, which is true on the first millimetres of the nonlinear crystal where parametric amplification is still weak, the coupled-amplitude equations describing difference frequency generation are:

$$\begin{cases} \frac{dA_s(z)}{dz} = \frac{8\pi j\omega_s^2 d_{eff}}{k_s c^2} A_p A_i^*(z) e^{j\Delta k z} \\ \frac{dA_i(z)}{dz} = \frac{8\pi j\omega_i^2 d_{eff}}{k_i c^2} A_p A_s^*(z) e^{j\Delta k z} \end{cases} \quad (2)$$

where $\Delta k = k_p - k_s - k_i$

Propagation equation of the idler wave is:

$$\frac{d^2 A_i(z)}{dz^2} = \kappa_s^* \kappa_i |A_p|^2 A_i(z) \quad (3)$$

with $\kappa_m = \frac{8\pi j\omega_m^2 d_{eff}}{k_m c^2}$. A similar equation can be written for the signal wave.

Maximum power conversion is achieved for perfect phase-matching condition, i.e. $\Delta k = 0$.

This system of equations can be solved, in the case of an unseeded idler wave $A_i(0) = 0$, into:

$$\begin{cases} A_s(z) = A_s(0) \cosh(\sqrt{\kappa_s \kappa_i} |A_p|^2 z) \\ A_i(z) = \frac{\kappa_i A_p(0)}{\sqrt{\kappa_s \kappa_i} |A_p|^2} A_s^*(0) \sinh(\sqrt{\kappa_s \kappa_i} |A_p|^2 z) \end{cases} \quad (4)$$

These solutions correspond to a signal field that keeps its initial phase-offset, and is simply amplified by the interaction, while the idler wave phase-offset depends on both the pump wave's and the signal wave's.

$$\varphi_i = \varphi_p - \varphi_s + \frac{\pi}{2} \quad (5-a)$$

Similarly, in the QPM case, high conversion efficiency can be achieved in a periodically poled crystal. The relation between the phases of the pump, signal and idler waves can be obtained propagating the waves in the crystal, domain by domain and step by step:

$$\varphi_i = \varphi_p - \varphi_s \quad (5-b)$$

Due to this phase relation, controlling the pump wave phase gives complete control of the idler wave phase. For instance, in the QPM case, a φ_{p0} phase shift induced on the pump wave will compensate for an idler wave phase variation of $\varphi_{p0} - \varphi_{s0}$, where φ_{s0} is the initial phase of the signal wave at the entrance of the nonlinear crystal.

Consequently, phase control of DFG and OPO converters is achievable, using all-fiber electro-optic phase modulators to control the pump wave.

We demonstrated experimentally the feasibility of such indirect phase control combining two DFG modules pumped by 1.064- μm Yb: fiber lasers delivering up to 15 W power each (see Fig. 1).

To fix and maintain the signal wavelength and phase, it is necessary to seed the DFGs with a signal seed at 1553 nm from a laser diode amplified by a commercial erbium-doped fiber amplifier split in two. Using this 1553-nm seeder, we are able to keep both DFG channels at a common and fixed signal wavelength.

The DFG nonlinear crystals are PPLN crystal from Covesion and their length is $L = 20$ mm. With a 1064-nm pump wavelength and a seeded signal at 1553 nm, quasi-phase matching in the PPLN crystal generates an idler wave at 3.4 μm . The pump beams are focused down to 100 μm waist in the PPLN crystals.

Coherent combining of these DFG modules is achieved using the idler waves interference signal to close the feedback loop (see Fig. 2).

Time-averaged combining efficiency is excellent: the residual phase error is ~ 28 rms for the idler wave.

This experiment is the proof that CBC of continuous wave DFG using indirect phase control is feasible, hence proving that OPO CBC is also feasible as the nonlinear process involved in both cases is the same: parametric amplification.

The main difference between SHG CBC and DFG CBC is that simultaneous phase locking that has been proved feasible for SHG combination [3], cannot be achieved so easily when combining non-degenerate three-wave mixing frequency

converters [5]. Even if seeded, the optical path difference between the two signal channels induces a phase difference that is not compensated for, and the signal waves are not phase-locked simultaneously when the idler waves are.

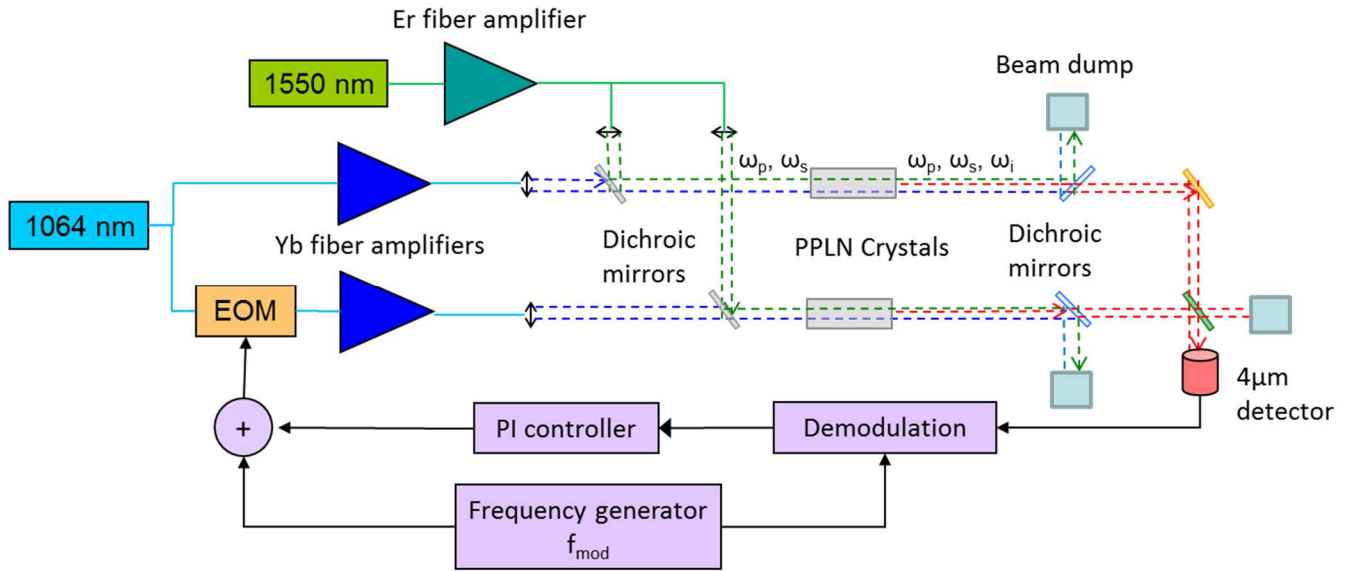


Figure 1. Schematics of the experimental set-up for demonstrating coherent combining of two 3.4- μm idler beams generated through DFG in PPLN crystals. Coherent combining is achieved by active phase-control of one of the pump waves.

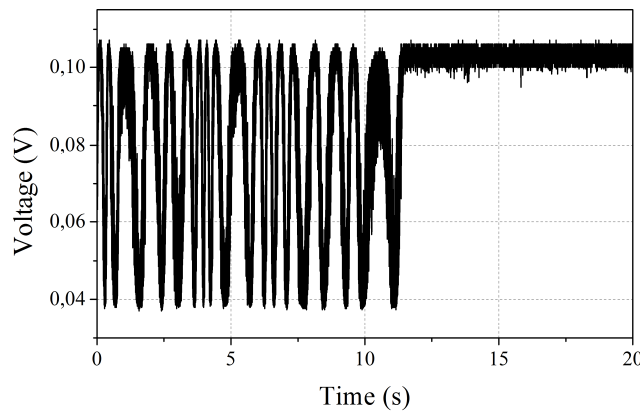


Figure 2. Time evolution of the interference signals of the idler beams when the phase control loop is open and then closed.

2.2 Experimental tests of OPO CBC, challenges and limitations

First step of experimentally combining OPOs was to design an efficient continuous-wave OPO cavity. Different cavities were tested, ring cavities and linear ones, and the best results were obtained with the linear cavity presented in Fig. 3 that offered the lowest emission threshold.

The cavity is 20-cm long and is formed between two concave mirrors with 50-mm and 130-mm curvature radius respectively. Both are high reflection coated for the signal wavelength at 1.5 μm ($R_s > 97\%$) and the output coupler is high transmission at the idler midinfrared wavelength. Both mirrors offer a low reflection at the pump wavelength to minimize the pump losses.

With this linear cavity, the OPO threshold was around 7 - 8 W and the OPO delivered a few hundreds of milliwatts of idler power at 3.8- μm wavelength as can be seen in Fig. 4.

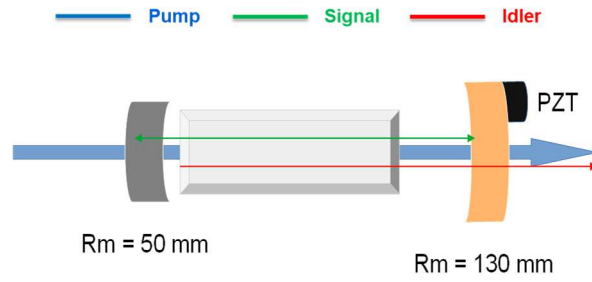


Figure 3. Optimal continuous-wave OPO linear cavity. The output coupler is mounted on a piezo-electric translation stage to be able to finely tune the position of the spectrum emitted.

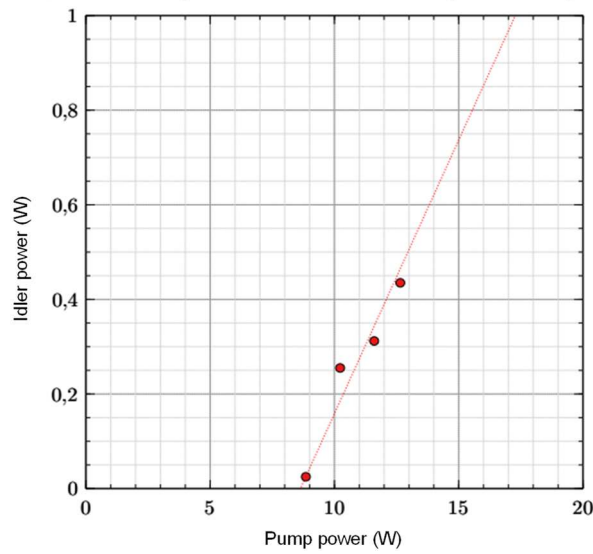


Figure 4. Idler power vs. pump power for the continuous-wave OPO..

After duplicating the cw OPO cavity, we began testing CBC of OPOs. The experimental setup is arranged as in Fig. 5.

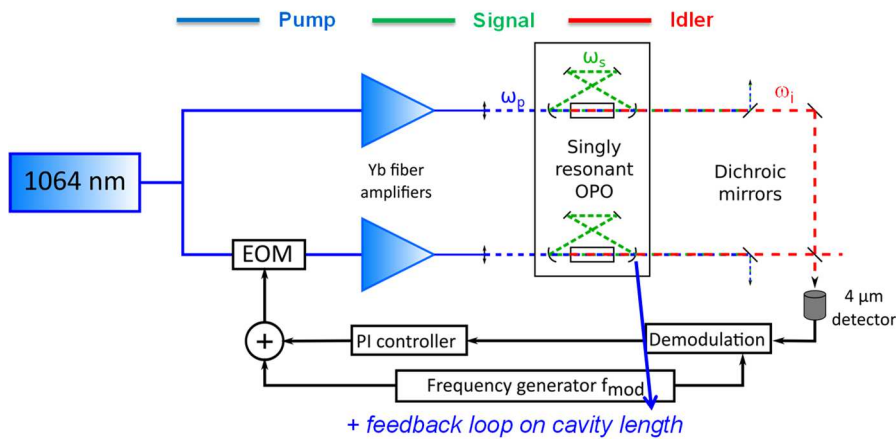


Figure 5. OPO CBC experimental setup. For the sake of making the figure easier to read, ring cavities are drawn for the OPOs but we used the optimized linear cavity for both OPOs in the experiment.

Using a wavemeter and finely tuning the temperature of the second NL crystal, we were able to bring the second signal wavelength very close to the first one, sufficiently close to allow for fine adjustment of the second signal wavelength to the other signal wavelength value using cavity length tuning with a piezo-electric micro-positioner.

Unfortunately, even with a singly-resonant OPO that should provide smooth tuning of the signal wavelength with the cavity length, we observed thermally induced longitudinal mode-hops that made it impossible to implement proper feedback on the signal wavelength through cavity length control.

Parasitic Fabry-Perot effect due to residual reflectivity of the cavity mirrors at the pump wavelength were also observed and induced detrimental power fluctuations even after limiting their impact as much as possible.

Coherent combining of cw OPOs couldn't be achieved and would require a higher level of stabilization of the OPO cavities than the one available on the experimental setup, as well as a choice of mirrors specifically designed for the OPO cavity with higher transmittance for the pump wavelength.

3. TARGET-IN-THE-LOOP COHERENT COMBINING OF 7 FIBER LASERS

3.1 The laser testbed for CBC and TIL-CBC

The laser configuration is a standard 7-channel master oscillator power amplifier (MOPA) configuration at 1.5 μm wavelength. A single-frequency low power (40 mW) master oscillator (MO) is split and amplified into 7 channels. Each of the 7 Er-Yb doped fiber amplifiers delivers up to 3 W at 1543 nm. One of the fiber amplifiers is not phase controlled and is free to fluctuate in phase while in-between the MO and 6 of the amplifiers, we use fast electro-optic phase modulators with a 150-MHz bandwidth to control the phase of each channel and simultaneously tag each of these 6 channels at a specific frequency around 20 MHz with a low-depth phase modulation.

In this self-referenced LOCSET configuration, the 6 phase-controlled channels follow the phase fluctuations of the seventh channel that's not modulated (see Fig. 6).

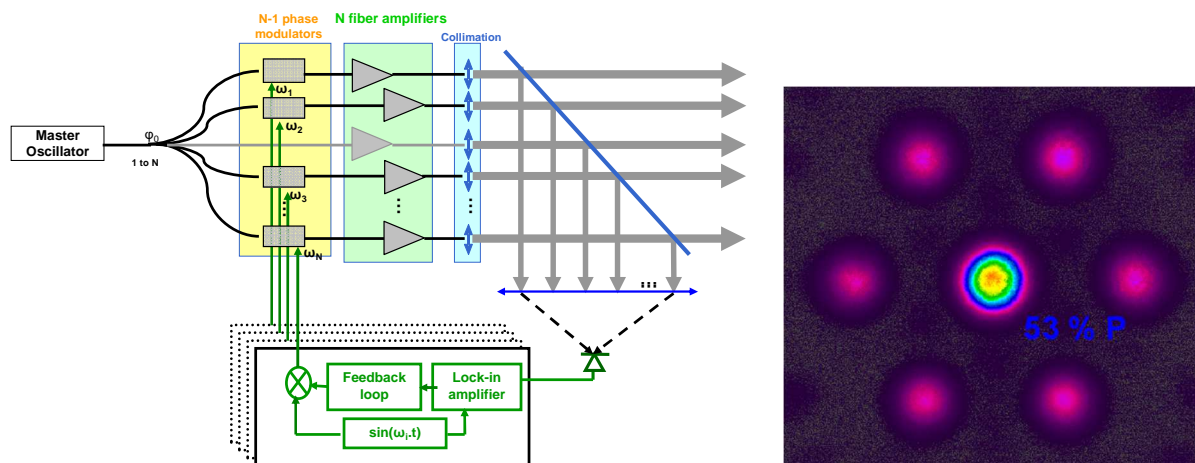


Figure 6. On the left side, schematics of the experimental setup for frequency-tagging CBC (also known as LOCSET). On the right side, interference pattern in the far-field, captured on a 1.5- μm camera located at the same distance as the direct CBC detector.

The 7-channel CBC setup delivers a nice interference pattern in the far-field. We confirmed that in direct CBC, i.e. using a fast photodiode to capture part of the central lobe of interference in the far-field, it was easy to lock the phases of the 7 laser channels and stabilize the position of the interference pattern.

In LOCSET, frequency tagging of the i^{th} channel at a specific frequency ν_i results in an interference signal that generates an error signal after demodulation at the same frequency given by equation:

$$i_{error_i}(t) \propto E_i J_1(\beta_i) \left[E_u \sin(\phi_u - \phi_i) + \sum_{j=1}^{N-1} E_j J_0(\beta_j) \sin(\phi_j - \phi_i) \right]$$

where ϕ_i is the i^{th} amplifier chain output phase in the photodetector plane, and ϕ_u the unmodulated reference beam phase in the photodetector plane. E_i and E_u are the respective electric field amplitudes at the output of the i^{th} amplifier and of the unmodulated amplifier. β_i and β_u are the respective modulation depths of the i^{th} amplifier channel and of the unmodulated channel. Driving the 6 error signals simultaneously to zero in real time results in maintaining equal phases for the 7 channels. Any sudden phase shift is immediately compensated for, thanks to the very fast electro-optic phase modulators and fast detection.

CBC efficiency measured as the fraction of the total power located in the central lobe of the interference pattern was higher than 53 % (see Fig. 6). It's very close to the experimental maximum that can be achieved with Gaussian laser beams (theoretical maximum is 63 %), but a little lower due to the opto-mechanical constraints limiting the effective fill-factor in the near-field.

Residual phase error has been measured and is lower than $\lambda/40$, confirming again the high efficiency of the CBC process and the high speed of the feedback loop. The opto-mechanical head where the outputs of the 7 fiber amplifiers are collimated and sent through the atmosphere is completely adjustable (see Fig. 7). Piezo-electric motors are used to set the transverse position of the output fiber tip with respect to the collimating lens, in order to align the 7 collimated beams in the same direction. The focus of the collimating lenses is manually tuned beforehand. Figure 3 presents pictures of the first part of the testbed dedicated to laser emission.

For Target-In-the-Loop Coherent Beam Combining (TIL-CBC), a second stage of the testbed is dedicated to long range focusing of the laser beams and to collection and detection of the backscattered signal from the remote target. We chose to use a bi-static configuration (see Fig. 8) where the long range focusing and the reception apertures are separated, to limit the risk of narcissus effect, and decrease the optical complexity of the detection line with respects to a monostatic configuration.

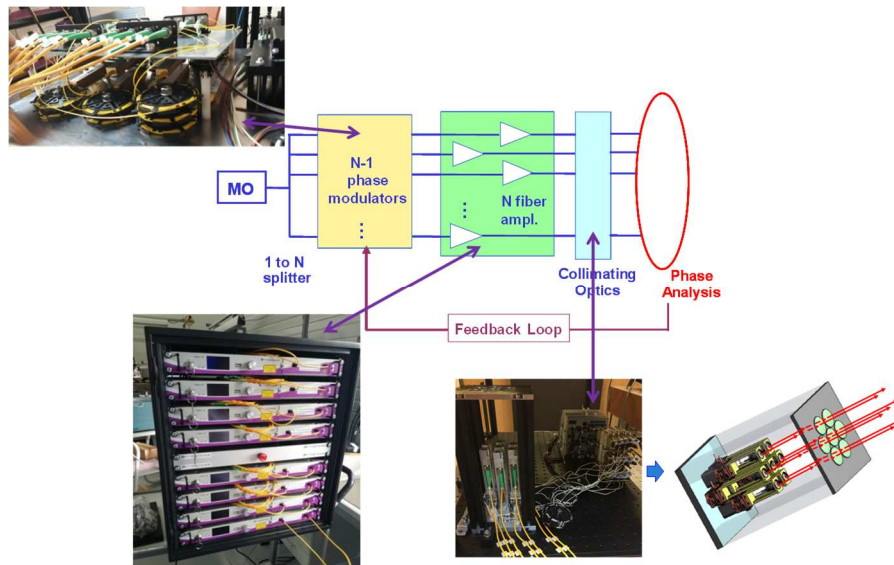


Figure 7. Pictures of the experimental setup parts.

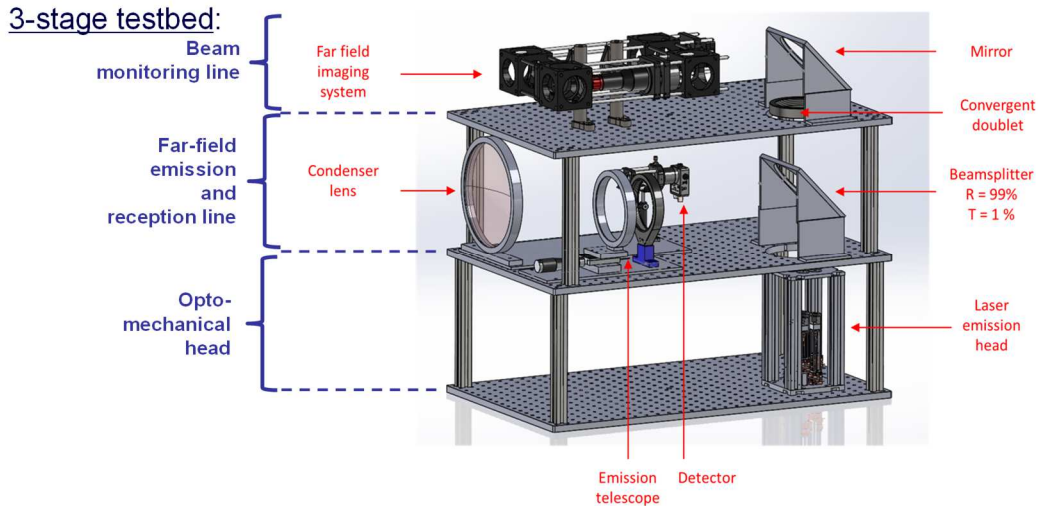


Figure 8. View of the complete testbed with both emission and reception lines.

3.2 Experimental demonstration of TIL-CBC

After some first demonstrations of CBC and TIL-CBC in the laboratory and then outdoor at shorter range (less than 100 m), the testbed that has been designed to be mobile was transferred to our laser site where we are able to shoot lasers safely up to 1-km range (see Fig. 9). The site is equipped with proper apparatus to monitor the weather and atmospheric conditions, and also to measure turbulence strength through the average value of the C_n^2 over 1 km.

The experiments took place during summer in the south west of France. As the laser beams propagated horizontally at 1.5 m from the ground, the level of turbulence was quite high and the average value of C_n^2 over 1 km was often close to or even much higher than $10^{-13} \text{ m}^{-2/3}$.

Despite these detrimental turbulence conditions, when the C_n^2 value was lower than $10^{-13} \text{ m}^{-2/3}$, we were able to perform efficient TIL-CBC up to 1 km.

A transparent wedge plate was placed before the target, to reflect a small fraction of the combined beams power to a black screen located at the same distance as the target. Proceeding like this, we could record video sequences of the interference pattern displayed on black screen and observed with an InGaAs Raptor camera, without interfering with the TIL-CBC process in the target plane. Fig. 9 presents instantaneous images of the interference pattern with and without closing the CBC feedback loop.

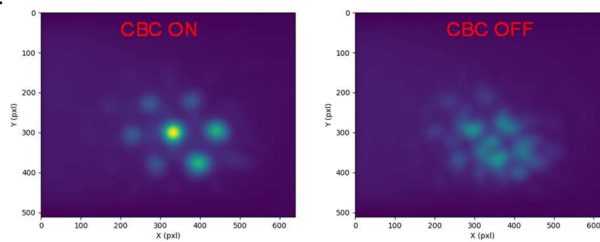


Figure 9. Instantaneous images of the interference pattern generated at 310 m when TIL-CBC feedback loop is active and inactive.

Fig. 10 presents averaged images from the same video sequence. The size of the interference lobes is not different in the instantaneous images and in the averaged image, demonstrating that the interference pattern was locked on a fixed position in the target plane.

Fig. 11 presents the averaged image obtained when target distance was 1 km.

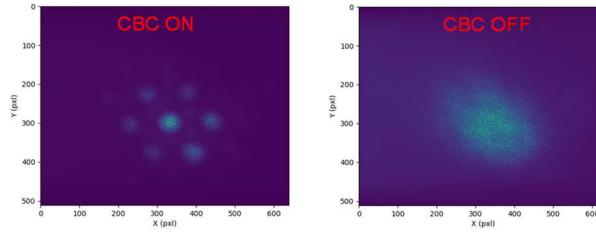


Figure 10. Averaged images of the interference pattern generated at 310 m when TIL-CBC feedback loop is active and inactive.

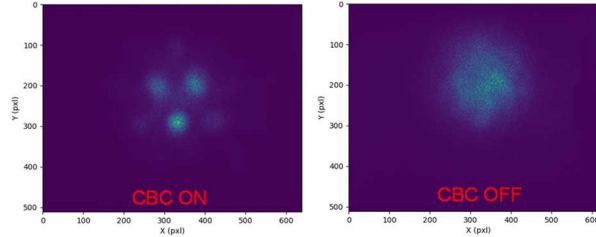


Figure 11. Averaged images of the interference pattern generated at 1 km when TIL-CBC feedback loop is active and inactive.

Even if turbulence induced perturbations clearly appear to decrease the efficiency of the CBC locking process, TIL-CBC still operates successfully and results in an increased power density deposited on the remote target at 1 km.

4. CONCLUSION

We developed an experimental setup for coherent combining of continuous wave OPOs with active phase control of their pump waves.

To prevent fluctuations of the intracavity pump power, parasitic Fabry-Perot effects on the pump wave have to be mitigated. Temperature tuning of NL crystal is enough to bring both signal wavelengths close enough for fine tuning through cavity length adjustment.

However, this experimental test of OPO coherent combining was unsuccessful due to detrimental signal cavity mode-hops that prevented from smooth enough tuning of the signal wavelength.

We also developed a mobile testbed for coherent beam combining of 7 fiber lasers emitting at 1.5 μm . This testbed operates through frequency-tagging phase difference monitoring. It can concentrate more than 53 % of the overall power in the central of the interference pattern generated in the far-field, after overlap of the laser beams.

The testbed has been designed to use the backscattered signal coming from a remote target as a reference for phase difference monitoring and phase locking. It was operated in a target-in-the-loop configuration, first at short distance in the laboratory, and then at longer distance outdoors, propagating the beams through real, weak to strong atmospheric turbulence.

The longer range outdoor experimental campaign demonstrated that TIL-CBC efficiency is preserved up to more than 310 m. Perturbations induced by strong atmospheric turbulence are significantly affecting TIL-CBC, but TIL-CBC operates successfully at 1-km range anyway, albeit with lower efficiency.

Future work is dedicated to modifying the testbed to improve its performances, especially when dealing with strong atmospheric turbulence conditions.

ACKNOWLEDGMENTS

This work was partially funded by French Delegation Generale pour l'Armement.

REFERENCES

- [1] Shekel, E., Vidne, Y. and Urbach, B., "16kW single mode CW laser with dynamic beam for material processing," Proc. SPIE 11260, 1126021 (2020).
- [2] Lombard, L., Azarian, A., Cadoret, K., Bourdon, P., Goular, D., Canat, G., Jolivet, V., Jaouen, Y. and Vasseur, O., "Coherent beam combination of narrow-linewidth 1.5 μm fiber amplifiers in a long-pulse regime," Opt. Lett. 36(4), 523-525 (2011).
- [3] Odier, A., Durécu, A., Melkonian, J-M., Lombard, L., Lefebvre, M. and Bourdon, P., "Coherent combining of second-harmonic generators by active phase control of the fundamental waves," Opt. Lett. 42(16), 3201-3204 (2017).
- [4] Odier, A., Durécu, A., Melkonian, J-M., Lombard, L., Lefebvre, M. and Bourdon, P., "Coherent combining of fiber-laser-pumped 3.4- μm frequency converters," Proc. SPIE 10083, 1008319 (2017).
- [5] Odier, A., Chtouki, R., Bourdon, P., Melkonian, J-M., Lombard, L., Godard, A., Lefebvre, M. and Durécu, A., "Coherent combining of mid-infrared difference frequency generators," Opt. Lett. 44(3), 566-569 (2019).
- [6] Bourderionnet, J., Bellanger, C., Primot, J. and Brignon, A., "Collective coherent phase combining of 64 fibers," Opt. Express 19(18), 17053–17058 (2011).
- [7] Chang, H., Chang, Q., Xi, J., Hou, T., Su, R., Ma, P., Wu, J., Li, C., Jiang, M., Ma, Y. and Zhou, P., "First experimental demonstration of coherent beam combining of more than 100 beams," Photon. Res. 8(12), 1943-1948 (2020).
- [8] Pearson, J. E. Bridges, W. B. Hansen, S. Nussmeier, T. A. and Pedinoff M. E., "Coherent optical adaptive techniques: design and performance of an 18-element visible multidither COAT system," French-German Institute of Saint-Louis (2013).
- [9] Weyrauch, T., Vorontsov, M. A., Carhart, G. W., Beresnev, L. A., Rostov, A. P., Polnau, E. E. and Jiang Liu, J., "Experimental demonstration of coherent beam combining over a 7 km propagation path," Opt. Lett. 36(22), 4455–4457 (2011).
- [10] Jolivet, V., Bourdon, P., Bennai, B., Lombard, L., Goular, D., Pourtal, E., Canat, G., Jaouen, Y., Moreau, B. and Vasseur, O., "Beam shaping of single-mode and multimode fiber amplifier arrays for propagation through atmospheric turbulence," IEEE J. Sel. Top. Quant. Elec. 15(2), 257–268 (2009).
- [11] Shay, T. M., Benham, V., Baker, J. T., Ward, B., Sanchez, A. D., Culpepper, M. A., Pilkington, D., Spring, J., Nelson, D. J. and Lu, C. A., "First experimental demonstration of self-synchronous phase locking of an optical array," Opt. Express 14(25), 12015–12021 (2006).